Journal of Trace Elements in Medicine and Biology 54 (2019) 62–68

Contents lists available at ScienceDirect

Journal of Trace Elements in Medicine and Biology

journal homepage: www.elsevier.com/locate/jtemb

Effects of platinum-based anticancer drugs on the trace element profile of liver and kidney tissue from mice

John T. Sloop[a], Jake A. Carter[a], Ulrich Bierbach[b], Bradley T. Jones[a], George L. Donati[a,*]

[a] Department of Chemistry, Wake Forest University, Salem Hall, Box 7486, Winston-Salem, NC, 27109, USA
[b] Department of Chemistry, Wake Forest University, Wake Downtown Campus, 455 Vine St., Winston-Salem, NC 27101, USA

ARTICLE INFO

Keywords:
Inductively coupled plasma mass spectrometry
Element homeostasis
Drug development
Multivariate analysis
Random forest importance
Cancer treatment

ABSTRACT

Background: Platinum-based anticancer drugs are relatively successful chemotherapeutic agents, which can cause significant elemental changes in key organs and are known for undesirable side effects, such as nephrotoxicity (damage to the kidneys).

Objectives and methods: Inductively coupled plasma mass spectrometry (ICP-MS) and traditional statistical tools such as two-sample Student's *t*-test and Pearson's correlation analysis are used to evaluate the effects of different investigational Pt-based anticancer drugs on the elemental constitution of kidneys and liver of mice. Principal component analysis is used to uncover relationships in element concentration and potential correlations between those and clinical effects. Random forest importance is used to identify elements most associated with the drug's maximum tolerated doses (MTDs).

Results: Strong negative correlations between Pt and both Cu (−0.814) and Zn (−0.784) in kidneys were observed for one of the Pt-acridine anticancer agents evaluated (Drug C). Strong positive correlations were observed between Cu in both kidneys (0.834) and liver (0.756) with Zn in liver for the same compound. Cisplatin administration correlates to higher concentrations of Ca, Cu, Rb and Zn in liver. Calcium and Mo in kidneys and Pt and Zn in liver are the features most associated with MTDs.

Conclusions: The results indicate that the Pt-based agents investigated are major modulators of ion homeostasis in excretory organs, which most likely contributes to their systemic toxicity and limits their efficacy. A better understanding of subtle patterns and correlations among elements in key organs may provide deeper insights into the mechanisms of action and ultimately contribute for better, safer drugs. To achieve this goal, researchers involved in cancer drug development may leverage the high sensitivity and high sample throughput of ICP-MS, and the capabilities of modern statistical tools to extract relevant information from a large dataset.

1. Introduction

Cisplatin, oxaliplatin, and carboplatin are well-known platinum-based chemotherapeutic drugs, whose mode of action has been linked to their ability to crosslink purine bases on DNA. These Pt-based drugs cause DNA damage by forming permanent adducts with nucleobases and, subsequently, induce apoptosis in cancer cells [1]. Despite their success at treating several types of solid tumors, there have also been numerous undesirable side effects linked to these drugs, such as nephrotoxicity (damage to the kidneys), neurotoxicity, and increased susceptibility to infections [1].

It has been demonstrated that some types of cancer are linked to variations in organ-specific concentrations of metal ions [2]. Zinc levels, for example, are reduced in carcinomas of the liver, gallbladder, digestive tract, and prostate [3]. Likewise, iron overload has been linked to various cancers, such as colorectal, liver, and kidney malignancies [4]. Pt-based anticancer therapeutics have been shown to affect various elements in a number of ways. Intracellular calcium ($[Ca^{2+}]_i$), for example, has been shown to increase after Pt-based anticancer therapy [5,6]. Cysteine-rich metallothioneins play an important role in detoxification and storage of various metals (*e.g.* Cd, Cu, Pb, Ni and Zn), and are overexpressed in response to treatment with Pt complexes, which, in turn, could lead to changes in element levels in the cells [7]. Cisplatin, one of the classical Pt-based anticancer drugs, changes the metabolism of Al, Ba, Cr, Ni, Pb and Sr, in addition to inhibiting Rb uptake into the cytoplasm [8]. The reduction of Rb^+ uptake, for

Abbreviations: ICP-MS, inductively coupled plasma mass spectrometry; PCA, principal component analysis; RFI, random forest importance; MTD, maximum tolerated dose; CRM, certified reference material; LOD, limit of detection

* Corresponding author.
E-mail address: donatigl@wfu.edu (G.L. Donati).

https://doi.org/10.1016/j.jtemb.2019.04.005
Received 15 January 2019; Received in revised form 9 April 2019; Accepted 11 April 2019

instance, is caused by inhibition of the Na^+/K^+-ATPase ion pump, which is also a likely contributing factor to the nephrotoxicity of cisplatin [9]. To elucidate the consequences of cancer-specific alterations in cell metabolism and the effects of Pt-based cancer therapies on essential and nonessential trace elements, more efficient analytical methods are required to improve our understanding of disease pathology and to potentially devise personalized treatment options.

Inductively coupled plasma mass spectrometry (ICP-MS) allows for high sensitivity and high sample throughput in applications involving a wide range of elements and in a broad variety of sample matrices. Its ability to quantify metals at the parts per billion (μg/L) and parts per trillion (ng/L) levels makes it a powerful tool for trace element analysis of biological samples [10]. Recent applications also include methods to support drug development, as ICP-MS can provide quantitative information on the drug itself and possible metabolites, as well as the number, nature, and concentration of impurities, which, in turn, allows for significant improvements in drug safety and product quality [11]. In this context, ICP-MS has been used as a valuable tool for the determination of drug-related platinum in biological fluids and tissues at or below the parts per billion level [12].

While large amounts of data can be obtained with ICP-MS, utilizing its full potential to gain insight into complex processes and networks in biological systems is an unexplored application. For example, the multi-element capabilities of ICP-MS can be used to determine a specific element's relationship to other various elements in a sample to better understand a biological process. However, multi-element methods generate a large amount of data, for which processing and interpreting can prove extremely challenging. Recently, various advanced statistical techniques have been developed to tackle such challenges and allow for the extraction of underlying information in a large dataset [13,14]. Some examples of such multivariate statistical tools include principal component analysis (PCA) and random forest importance (RFI) determination [13–16].

PCA is a useful visualization tool with applications in finance, neuroscience, and multi-elemental fingerprinting [13,16–18]. Data is broken down into what is known as principal components (PCs), and each PC is responsible for a percentage of variability in the sample population. In a two-axis PCA plot, which usually includes the first couple of PCs, one can then visualize how (scores) and why (loadings) samples are related. In RFI determinations, which are based on random forest statistical models, feature (element) importance is determined based on the *gini* index [19]. In this case, the significance of a feature is related to a tree and a split in the ensemble of trees. A parameter, gVI_j (Eq. (1)), is obtained, which measures the importance of feature j from summing over the nodes containing feature j in tree k [20]. The higher the value for gVI_j the better the feature in splitting the data, and the more significant that feature is.

$$gVI_j = \frac{1}{ntree}\sum_{k=1}^{ntree} gVI_{jk} \quad (1)$$

In the current study, quantification of trace elements by ICP-MS in organs removed from test animals was combined with traditional statistical tools, such as the two-sample Student's *t*-test and Pearson correlation analysis. The goal was to evaluate the effects of the anticancer drug cisplatin and three nonclassical platinum-(benz)acridine (notations P#A# and P#B#) anticancer agents on the levels of selected trace elements in the kidneys and liver of necropsied mice. The three hybrid agents were selected from previously synthesized libraries: P17-A1 (Drug A), a lipophilic valproic ester prodrug [21]; P3-B1 (Drug B), a DNA structure-selective and less cytotoxic derivative [22], and P8-A1 (Drug C), the most cytotoxic and efficacious agent identified to date [21]. PCA was then used as an exploratory tool and visual aid to uncover relationships in element concentration and observe potential correlations between those and clinical effects. RFI was used to identify the elements most associated with the drug's maximum tolerated doses (MTD), which is a general measure of systemic toxicity.

Table 1
ICP-MS operating conditions for CRM, and kidneys and liver sample analysis.

Instrumental parameter	Operating condition
Plasma	
Radio frequency applied power (W)	1550
Sampling depth (mm)	10.0
Carrier gas flow rate (L/min)	1.07
Peristaltic pump rate (rps)	0.10
Collision/reaction cell	
H_2/He gas flow rate (mL/min)	4.0/3.5
Octopole bias (V)	−18.0
Octopole RF (V)	19.0
Energy discrimination (V)	5.0
Other analytical parameters	
Mass spectrometer mode	Single quadrupole
Integration time (s)	0.1
Number of sample replicates	3
Analytes (mass-to-charge ratios, *m/z*)	
Ca (40), Cd (111), Cu (63), Mn (55), Mo (95), Pt (195), Rb (85), Se (78), Sr (88), Zn (66)	

2. Materials and methods

2.1. Instrumentation

All element determinations were performed using a tandem quadrupole ICP-MS (ICP-MS/MS, Agilent 8800, Agilent, Tokyo, Japan). Three separate collision/reaction cell gases were evaluated to improve accuracy in ICP-MS/MS determinations: H_2, O_2, and He. The instrumental operating conditions were optimized for best percent recoveries of all analytes in comparison to certified concentration values in a certified reference material (CRM) of Bovine Liver. The optimized ICP-MS operating conditions and analyte mass-to-charge ratios (m/z) used in this study are listed in Table 1. A closed-vessel microwave-assisted digestion system (ETHOS UP, Milestone, Sorisole, Italy) was used for sample digestion.

2.2. Reagents and standard reference solutions

High-purity distilled-deionized water (Ultrapure Type 1) obtained from a Millipore Direct-Q® 3UV-R (Merck Millipore, Burlington, MA, USA), and trace-metal grade nitric acid and hydrochloric acid (Fisher, Pittsburgh, PA, USA) were used to prepare all calibration standards and samples. All solutions were prepared in 4% v/v acid (2% v/v HNO_3, 2% v/v HCl), with calibration standards obtained by dilution of single-element stock solutions of Ca, Cd, Cu, Mn, Mo, Pt, Rb, Se, Sr and Zn (1000 mg/L, High-Purity Standards, Charleston, SC, USA). The external standard calibration method was used in all determinations.

2.3. Samples

A CRM of Bovine Liver (NIST 1577b) from the National Institute of Standards and Technology (NIST, Gaithersburg, MD, USA) was used for method development and accuracy evaluation. The elements chosen for this study were Ca, Cd, Cu, Mn, Mo, Rb, Se, Sr and Zn, which was based on both known importance in cellular processes and previous studies associated with Pt-drug effects on element profile in tissues/cells [3,5–9,23,24]. Platinum was also determined in all samples. In this case, aliquots of digested liver samples were used in addition and recovery experiments to evaluate the method's accuracy for determining Pt.

Batches of platinum-(benz)acridines (Drugs A, B and C) of analytical purity greater than 95% have been synthesized and fully characterized previously [21,22]. Cisplatin (USP reference standard) was purchased from Sigma Aldrich. The structures of all four compounds evaluated in

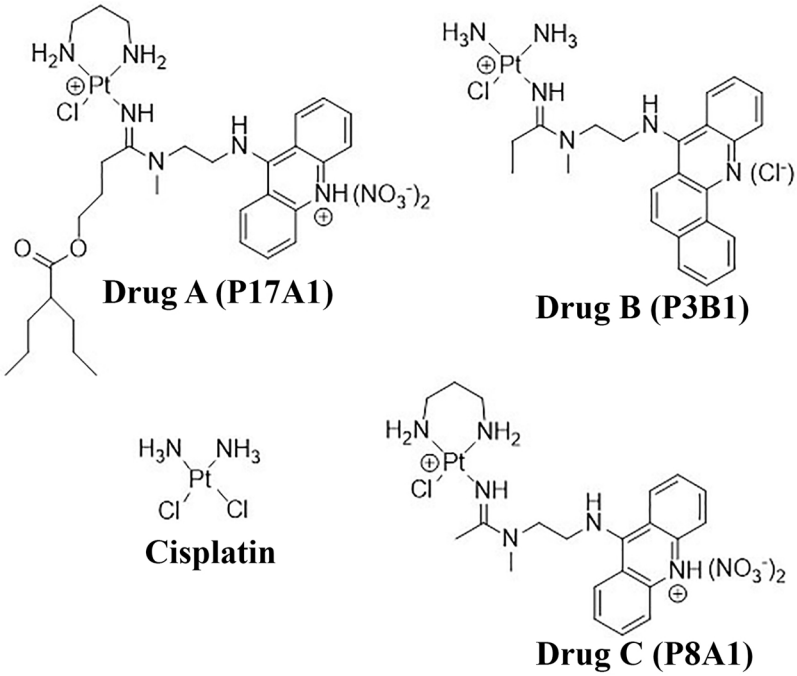

Fig. 1. Structures of cisplatin and the three non-classical Pt-acridine anticancer agents evaluated. Drug A (P17-A1) is a lipophilic valproic ester prodrug. Drug B (P3-B1) is a DNA structure-selective and less cytotoxic derivative. Drug C (P8-A1) is the most cytotoxic and efficacious agent when compared to the other drugs in this study.

Table 2
ICP-MS method accuracy and collision/reaction cell gases used for Ca, Cd, Cu, Mn, Mo, Pt, Rb, Se, Sr and Zn determinations.

Element	Collision/reaction cell gas	Recovery (%)[a]
Ca	H_2	90
Cd	He	98
Cu	H_2	99
Mn	H_2	97
Mo	He	92
Pt	He	90[b]
Rb	H_2	90
Se	H_2	95
Sr	He	90
Zn	He	97

[a] Percent recovery from certified or reference value in Bovine liver (NIST 1577b).

[b] Percent recovery from spiking experiment carried out with a digested liver sample from the control group.

this study are presented in Fig. 1. Liver and kidney tissue samples from two anti-tumorigenic activity studies in nude mice were provided by an outside contractor (Washington Biotechnology, Inc., Baltimore, MD, USA). Maximum tolerated doses (MTD, [mg drug/kg mouse weight]) were determined in Swiss Webster mice after intraperitoneal (Drugs A and B) or intravenous (Drug C) injection using dose escalation studies. Mice tolerated multiple doses (days 0, 4, 8, 12) without signs of major clinical toxicity and without significant weight loss at 1.6 mg/kg (Drug A), 3.2 mg/kg (Drug B), and 0.4 mg/kg (Drug C). A total of 5–7 animals per treatment group were housed, dosed with test compounds, and euthanized according to SOPs. The route of administration (ROA) for Drug C (0.4 mg/kg) was by intravenous (IV) injection, while Drug A (2 mg/kg), Drug B (4 mg/kg), and cisplatin (4 mg/kg) were injected intraperitoneally (IP). Treatment at the indicated doses, which were close to the respective MTDs determined for Drugs A, B and C, occurred on days 0, 4, 8, and 12 (q4d × 4) for the treated and control groups. Animals receiving cisplatin were dosed @ q4d × 15 up to day 56. At the conclusion of the studies, all mice were euthanized and organs collected and stored at −80 °C.

2.4. Sample preparation

The same digestion procedure was used for all mice liver and kidney samples, as well as the CRM. A 10 mL aliquot of a 20% v/v acid solution (10% v/v HNO_3, 10% v/v HCl) was added to approximately 100–500 mg of sample into a polytetrafluoroethylene (PTFE) digestion vessel. The microwave-assisted digestion program used included a 15 min ramp to reach 200 °C, and a 15 min hold step at 200 °C. After the digestion was complete, a 15 min cool down period was observed before opening the digestion vessels. Digested samples and blanks were then diluted with distilled-deionized water to a final acid concentration of 4% v/v prior to ICP-MS analysis.

3. Results and discussion

3.1. Accuracy and limits of detection of the ICP-MS method

The accuracy of the ICP-MS method was evaluated by analyzing a CRM of Bovine Liver (NIST 1577b). Because this material presents no certified values for Pt, an addition and recovery experiment using aliquots of digested liver samples from the control group was also performed. The best results and the respective collision/reaction cell gases used are detailed in Table 2. Adequate accuracies were found for all analytes evaluated, with recoveries in the 90–99% range. The instrumental limits of detection (LODs) were calculated according to IUPAC recommendations as three times the standard deviation of the blank (S_{blank}, n = 15) divided by the calibration curve slope (m), *i.e.* LOD = S_{blank}/m. The blank solution in this case is a 4% v/v acid solution (2% v/v HNO_3, 2% v/v HCl). The LOD values calculated for Ca, Cd, Cu, Mn, Mo, Pt, Rb, Se, Sr and Zn were 8, 0.03, 6, 0.8, 0.2, 0.007, 0.09, 0.5, 0.3 and 2 µg/L, respectively. According to the sample preparation procedure described earlier, these values correspond to 800, 3, 600, 80, 20, 0.7, 9, 50, 30 and 200 µg/kg, respectively, considering a 500 mg sample aliquot.

3.2. Effect of platinum-based anticancer drugs on element distribution in kidneys and liver

As expected, Pt was found in kidneys and liver of treated animals for all anti-tumorigenic drugs evaluated (Table 3). Differences in Pt

Table 3
Element concentrations (mean ± 1 standard deviation, μg/kg) in kidneys and liver of animals treated with Drug A, Drug B, Drug C, and cisplatin.

Analyte, organ	Drug A (n = 2)	Drug B (n = 5)	Drug C (n = 7)	Cisplatin (n = 8)
Ca, kidneys	48500 ± 200	35200 ± 6300	19600 ± 5600	12100 ± 1500
Ca, liver	31900 ± 5300	32400 ± 13100	40500 ± 6800	39600 ± 3700
Cd, kidneys	14.5 ± 5.6	15.8 ± 4.0	7.10 ± 4.43	8.87 ± 1.04
Cd, liver	6.34 ± 1.63	6.28 ± 0.72	< LOD	4.96 ± 0.94
Cu, kidneys	3990 ± 510	3380 ± 140	1830 ± 200	1900 ± 110
Cu, liver	2680 ± 230	3040 ± 160	2900 ± 330	3400 ± 180
Mn, kidneys	1160 ± 30	1020 ± 190	788 ± 199	682 ± 87
Mn, liver	1000 ± 50	914 ± 54	890 ± 61	750 ± 96
Mo, kidneys	369 ± 66	346 ± 58	218 ± 68	287 ± 12
Mo, liver	858 ± 32	706 ± 89	715 ± 66	779 ± 54
Rb, kidneys	5420 ± 580	3610 ± 250	6760 ± 930	5680 ± 550
Rb, liver	6580 ± 10	5430 ± 330	7660 ± 790	8290 ± 540
Se, kidneys	1650 ± 180	1450 ± 100	1600 ± 530	1410 ± 230
Se, liver	1330 ± 60	1330 ± 110	386 ± 47	398 ± 24
Sr, kidneys	< LOD	< LOD	< LOD	< LOD
Sr, liver	< LOD	< LOD	32.2 ± 10.2	31.9 ± 8.8
Pt, kidneys	130 ± 30	940 ± 230	140 ± 80	1380 ± 510
Pt, liver	451 ± 131	2220 ± 320	290 ± 60	1360 ± 700
Zn, kidneys	14800 ± 3000	11900 ± 600	13200 ± 1200	12500 ± 300
Zn, liver	15300 ± 500	17900 ± 1300	21800 ± 2000	23500 ± 1900

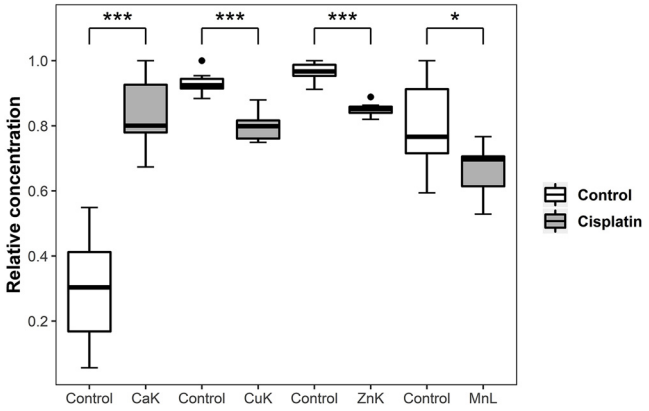

Fig. 2. Differences in elemental concentrations between the control and cisplatin-treated groups. Each "Control" group on the *x*-axis corresponds to its respective element on the right. CaK, CuK, ZnK and MnL correspond to Ca, Cu and Zn in kidneys, and Mn in liver, respectively. The relative concentrations on the *y*-axis were calculated for each control/drug-treated pair by dividing each individual value by the maximum concentration found within the pair. Statistical significance, based on a two-sample Student's *t*-test, is identified as *, **, or *** for $p <$ 0.05, 0.01, or 0.001, respectively.

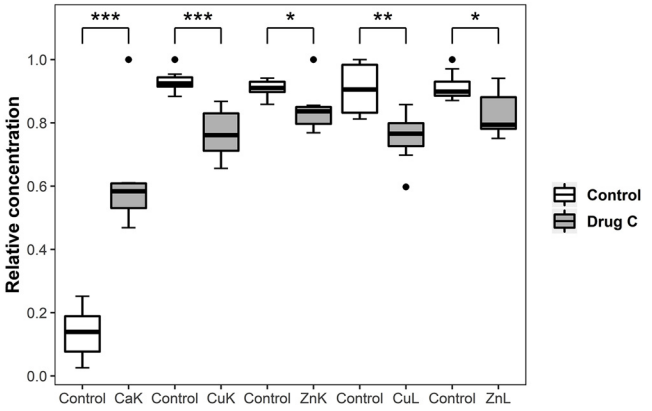

Fig. 3. Differences in elemental concentrations between the control and Drug C-treated groups. Each "Control" group on the *x*-axis corresponds to its respective element on the right. CaK, CuK, ZnK, CuL and ZnL correspond to Ca, Cu and Zn in kidneys, and Cu and Zn in liver. The relative concentrations on the *y*-axis were calculated for each control/drug-treated pair by dividing each individual value by the maximum concentration found within the pair. Statistical significance, based on a two-sample Student's *t*-test, is identified as *, **, or *** for $p <$ 0.05, 0.01, or 0.001, respectively.

concentration may be related to the specific dosing and administration regimes, which depended on drug toxicity. The most intense and variated effects (two-sample *t*-test at the 95% confidence level) for the other trace elements were observed for Drug C. When compared with the control group, Ca and Rb levels were 350% and 17% higher in the kidneys of treated animals, while Cu, Mo and Zn dropped by 18%, 28% and 7%, respectively. Concentrations of Cd, Cu, Rb and Zn in liver tissue decreased by 58%, 17%, 15% and 9%, with Sr levels increasing by 65%. Animals treated with cisplatin presented statistically significant differences (two-sample *t*-test at the 95% confidence level) in Ca, Cu, Mo and Zn in kidneys, and Mn and Sr in liver when compared with the control group. Calcium levels in the kidneys increased 178%, while Cu, Mo and Zn decreased 14%, 5% and 12%, respectively. Manganese and Sr variations in the liver were -18% and +64%, respectively, when compared with the control group. Figs. 2 and 3 show boxplots with effects of cisplatin and Drug C on the concentrations of some essential elements in the kidneys and liver.

Statistically significant differences in Ca, Cu, Mn, Rb and Se content in kidneys, and Sr content in liver were also observed between the control group and animals treated with Drug A. Concentration increases of 40%, 23%, 39%, 23% and 31% were observed for Ca, Cu, Mn, Rb and Se in kidneys, while Sr decreased 94% in liver. Finally, relatively fewer perturbations were observed for Drug B, with an 18% drop in Rb, and a 15% increase in Se in the kidneys of treated animals.

The differences in elemental concentrations in kidneys and liver of animals treated with Drug C and cisplatin, for example, may provide some clues to their distinct toxicity and efficacy. Fig. 4 shows the elements with statistically significant differences in concentration (two-sample *t*-test at the 95% confidence level) when comparing animals treated with these two drugs. Treatment with Drug C resulted in higher absolute Ca concentrations and a larger relative increase in Ca levels *versus* control in kidney tissue compared with cisplatin. This is an important observation since renal transporter-mediated extrusion into the urine is the major excretory mechanism of Pt-based drugs. Oxidative stress conditions caused by metallodrugs lead to dysfunctional ion homeostasis and elevated levels of cytoplasmic Ca^{2+} ions [25]. These conditions lead to downstream events causing necrotic or apoptotic death of renal proximal tubule cells, which is considered a major cause of nephrotoxicity. The fact that platinum from Drug C, although present in the kidneys at significantly lower residual levels than that from

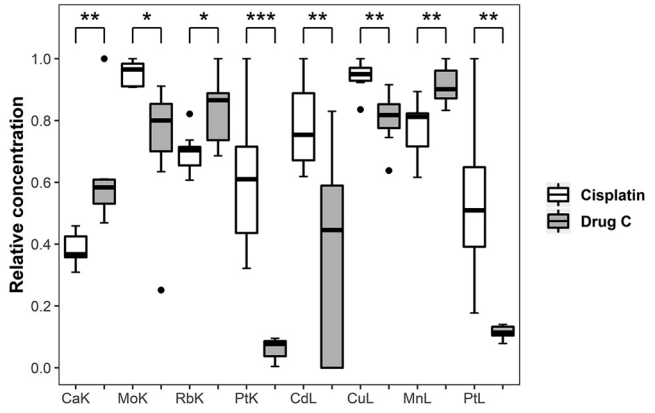

Fig. 4. Elements with statistically significant differences (two-sample Student's *t*-test at the 95% confidence level) between animals treated with cisplatin and Drug C. CaK, MoK, RbK, PtK, CdL, CuL, MnL and PtL correspond to Ca, Mo, Rb and Pt in kidneys, and Cd, Cu, Mn and Pt in liver. The relative concentrations on the *y*-axis were calculated for each cisplatin/Drug C-treated pair by dividing each individual value by the maximum concentration found within the pair. Statistical significance is identified as *, **, or *** for $p < 0.05$, 0.01, or 0.001, respectively.

cisplatin, causes substantial accumulation of Ca in this tissue suggests that this particular ion imbalance may be a major contributor to the higher systemic toxicity of this platinum-acridine hybrid agent when compared with cisplatin.

Although hepatotoxicity is usually not considered a significant cause of adverse effects associated with platinum drugs, we have also evaluated the effects of our test compounds on element levels in liver tissue. Copper, Rb and Zn levels in this organ showed the largest decrease in treated animals relative to control. Several mechanisms may contribute to the loss of these ions, which may reflect enhanced extrusion or reduced absorption. These include competitive displacement of metal ions from storage proteins, such as metallothioneins, as a form of intracellular ion mobilization, or reduced membrane permeation of these ions due to direct interactions of Pt with ATP-dependent and independent membrane transporters [9].

One potential use of ICP-MS data (and more broadly trace element levels) in anticancer drug development is the characterization of correlations between element concentrations in different organs at specific time points during treatment, and mechanistic features, efficacy, and systemic toxicity in *in vivo* models. Several evident differences have emerged with regard to the effects of the specific chemotypes. As demonstrated in Fig. 5, Drug C shows a broader range of statistically significant element concentration correlations (represented by the Pearson correlation coefficient). For example, there are strong negative correlations between Pt and both Cu and Zn in the kidneys when this drug is employed. A similar correlation coefficient is observed between Pt and Zn in the kidneys for cisplatin, but no correlation is observed between Pt and Cu in the same organ. Some additional interesting correlations are the ones between Cu in both kidneys and liver with Zn in liver for Drug C.

3.3. PCA and RFI to identify elements associated with a specific pharmacophore

The concentrations of elements in the sample solutions ranged from ng/L to mg/L. They were all normalized according to sample mass and expressed in μg/kg of the original solid sample. Concentration values from all 10 analytes (Table 3) were used in combination with PCA to provide a broader, multivariate visualization of the effects of all four drugs on the homeostasis of elements in kidneys and liver. Because PCA is sensitive to the scale of data, features (*i.e.* element concentrations) were normalized to a mean of 0 and standard deviation of 1 [26]. From all 20 original features (10 analytes in each organ), however, only 18 were used for PCA and RFI. If an observation (sample) presented a feature with a value below the LOD, the LOD value for that feature was imputed. This was repeated for all features with more than 50% of observations above the respective LODs. Features with less than 50% of observations above the LOD were not considered for multivariate analyses. Therefore, SrK and SrL (Sr concentration values in kidneys and liver, respectively) were discarded when performing multivariate analyses, as most samples presented Sr levels below the LOD. The statistical language R and the *randomForest* and *Caret* packages were used to develop code for all data analysis techniques, which is available upon request [19,27].

PCA may be used to identify variations in specific elements and potentially correlate them to clinical observations for the drug itself. Such approach may contribute to a more global understanding of the pharmacological processes involved with each drug, including mechanisms of action and potential side effects. For the compounds evaluated in this study, for example, Drug A has been shown very toxic, causing sudden death of the animals (hence the limited number of replicate data, n = 2, as the experiment was terminated earlier). On the other hand, cisplatin has shown relatively low toxicity, but also relatively low efficacy, and Drug C was the most efficient at reducing tumor size even with relatively low doses when compared to the other compounds. Fig. 6 shows the results from PC1 and PC2, which together explain 62% of the variation in the data and identify the elements responsible for each drug group separation. As it can be observed by the vector directions in this figure, Drug A is related to higher concentrations of Ca in kidneys and Mn in kidneys and liver; cisplatin administration correlates to higher concentrations of Ca, Cu, Rb and Zn in liver; while Rb and Zn are found in higher concentrations in kidneys of animals treated with Drug C. It is important to note that explaining these correlations and their relationship with clinical effects is outside the scope of the present study. However, it becomes clear that the combination of advanced statistical techniques such as PCA and multi-element analysis may be used to evaluate the effects of Pt-based anticancer drugs on elemental homeostasis, and potentially correlate a drug systemic toxicity and/or efficacy with elemental levels in key organs such

Drug A	RbK
CuK	0.997 (*)

Drug B	SrL	PtL
RbK	0.826 (*)	-
PtK	-0.884 (*)	0.931 (**)
PtL	-0.954 (**)	-

Drug C	MoK	PtK	CdL	RbL	ZnL
CaK	-0.908 (**)	-	-	-	-
CuK	-	-0.814 (*)	0.924 (**)	0.936 (***)	0.834 (*)
ZnK	-	-0.784 (*)	-	-	-
PtK	-	-	-0.818 (*)	-0.892 (**)	-
CdL	-	-	-	0.842 (**)	0.769 (*)
CuL	-	-	-	-	0.756 (*)

Cisplatin	ZnK	PtK	SrL	PtL
CaK	-0.882 (**)	0.685 (*)	-	-
ZnK	-	-0.736 (*)	-	-0.745 (*)
PtK	-	-	0.711 (*)	0.846 (**)

Fig. 5. Statistically significant correlations, represented by the Pearson correlation coefficient, between element concentrations in kidneys and liver samples of animals treated with Drugs A–C, and cisplatin. "K" and "L" after the element symbol represent kidney and liver samples, respectively. Statistical significance is identified as *, **, or *** for $p < 0.05$, 0.01, or 0.001, respectively.

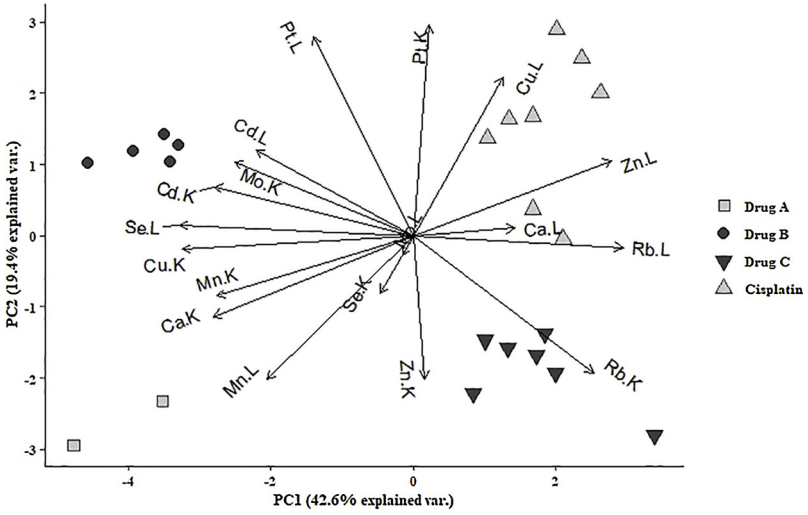

Fig. 6. Principal component analysis (PCA) biplot showing the four different drug groups and the elements responsible for group separation. "K" and "L" after the element symbol represent kidney and liver samples, respectively. The first two principal components (PC1 and PC2) explain 62% f the variance in the data, with good separation of the four drug groups. At no point during sample processing were the groups identified, which is typical of an unsupervised statistical method such as PCA.

as kidneys and liver.

RFI, based on random forest statistical models, is another powerful strategy for identifying subtle patterns in the data and potential correlations between clinical observations and elemental homeostasis in animal tissue [16,19]. In the present study, it has been used to rank the elements according to their importance on splitting the data into different levels of MTDs for Drugs A–C and cisplatin. The features were ordered according to *gini* importance and scaled against the highest ranking feature. In this case, three classification levels of MTD were employed in the RFI model: low (0.4 mg/kg, Drug C), intermediate (1.6 and 3.2 mg/kg for Drugs A and B, respectively), and high (6 mg/kg, cisplatin). Note that the lower the MTD, the higher the potential systemic toxicity of the drug. Fig. 7 shows that Ca and Mo in kidneys and Pt and Zn in liver are the features most correlated with MTDs, with Mn in kidneys and Se in liver also relevant. These results corroborate those from Fig. 6, especially for Ca, for which the respective vector in the PCA plot points away from the cisplatin cluster (with the highest MTD). Although the disruption of intracellular Ca homeostasis is involved in cisplatin-induced nephrotoxicity, and it has been shown that renal Ca accumulation occurs after cisplatin administration to rats [28,29], the results presented in Table 3, Figs. 6 and 7 suggest that this effect may be even more pronounced for the non-classical Pt-acridine hybrid agents evaluated (especially Drug A and Drug B) than for cisplatin.

4. Conclusions

The combination of multi-element analysis with traditional and advanced data-driven statistical tools increases the quantity and quality of information that may be used in drug development. PCA may be employed to identify trends in elemental homeostasis and contribute to minimizing toxicity during drug design and evaluation, while RFI can be used to specifically identify the elements most affected by the use of the anti-tumorigenic agent.

In the present study, it has been observed that elements such as Ca, Cu, Mn, Mo, Rb and Zn may be the most affected by cisplatin and the three nonclassical platinum-(benz)acridine anticancer agents evaluated. The results presented here indicate that these drugs are major modulators of ion homeostasis in excretory organs, which most likely contributes to their systemic toxicity and limits their efficacy. By leveraging the high sensitivity and high sample throughput of ICP-MS, combined with the capabilities of modern statistical methods to extract relevant information from a large dataset, researchers involved in drug development may be able to achieve a better understanding of subtle patterns and correlations among elements in key organs, which will

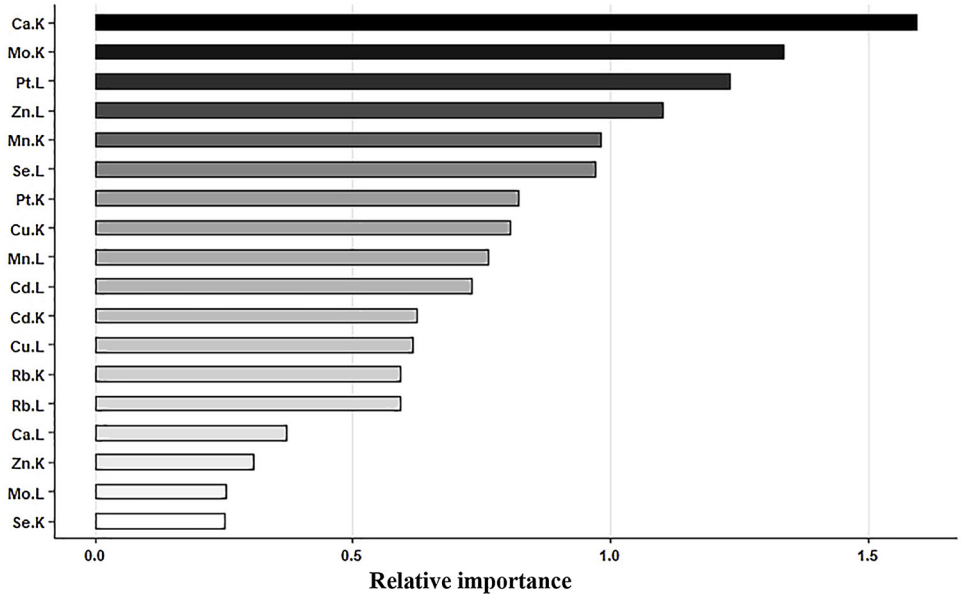

Fig. 7. Random forest variable importance to identify elements associated with maximum tolerated doses (MTDs). Elements are ranked according to their importance while splitting the data between low (0.4 mg/kg, Drug C), intermediate (1.6 and 3.2 mg/kg for Drugs A and B, respectively), and high (6 mg/kg, cisplatin) MTDs. Relative importance on the *x*-axis is based on node impurity as measured by the *Gini* index. "K" and "L" after the element symbol represent kidney and liver samples, respectively.

ultimately contribute for better, safer drugs.

Conflict of interest

All authors declare that there are no conflicts of interest associated with this manuscript.

Acknowledgements

This work was supported by the National Science Foundation's Major Research Instrumentation Program (NSF MRI, grant CHE-1531698). Funding for the animal studies was provided by the Wake Forest Innovation and Commercialization Services. We also thank the Department of Chemistry and the Graduate School of Arts and Sciences at Wake Forest University for their support.

References

[1] S. Dasari, P.B. Tchounwou, Cisplatin in cancer therapy: molecular mechanisms of action, Eur. J. Pharmacol. 740 (2014) 364–378, https://doi.org/10.1016/j.ejphar.2014.07.025.
[2] A. Sigel, H. Sigel, R.K.O. Sigel, Metal Ions in Toxicology: Effects, Interactions, Interdependencies, Walter de Gruyter GmbH, Berlin, 2011.
[3] M. Murakami, T. Hirano, Intracellular zinc homeostasis and zinc signaling, Cancer Sci. 99 (2008) 1515–1522, https://doi.org/10.1111/j.1349-7006.2008.00854.x.
[4] X. Huang, Iron overload and its associations with cancer risk in humans: evidence for iron as a carcinogenic metal, Mutat. Res. 533 (2003) 153–171, https://doi.org/10.1016/j.mrfmmm.2003.08.023.
[5] A. Muscella, N. Calabriso, C. Vetrugno, F.P. Fanizzi, S.A. De Pascali, C. Storelli, S. Marsigliante, The platinum (II) complex [Pt(O,O'-acac)(γ-acac)(DMS)] alters the intracellular calcium homeostasis in MCF-7 breast cancer cells, Biochem. Pharmacol. 81 (2011) 91–103, https://doi.org/10.1016/j.bcp.2010.09.012.
[6] A.M. Florea, D. Büsselberg, Anti-cancer drugs interfere with intracellular calcium signaling, Neurotoxicology 30 (2009) 803–810, https://doi.org/10.1016/j.neuro.2009.04.014.
[7] B. Desoize, C. Madoulet, Particular aspects of platinum compounds used at present in cancer treatment, Crit. Rev. Oncol. Hematol. 42 (2002) 317–325, https://doi.org/10.1016/S1040-8428(01)00219-0.
[8] K. Szentmihályi, Z. May, G. Szénási, C. Máthé, A. Sebestény, M. Albert, A. Blázovics, Cisplatin administration influences on toxic and non-essential element metabolism in rats, J. Trace Elem. Med. Biol. 28 (2014) 317–321, https://doi.org/10.1016/j.jtemb.2014.02.005.
[9] N.D. Eljack, H.M. Ma, J. Drucker, C. Shen, T.W. Hambley, E.J. New, T. Friedrich, R.J. Clarke, Mechanisms of cell uptake and toxicity of the anticancer drug cisplatin, Metallomics 6 (2014) 2126–2133, https://doi.org/10.1039/C4MT00238E.
[10] A. Montaser, Inductively Coupled Plasma Mass Spectrometry, Wiley-VCH, New York, 1998.
[11] D. Pröfrock, A. Prange, Inductively coupled plasma-mass spectrometry (ICP-MS) for quantitative analysis in environmental and life sciences: a review of challenges, solutions, and trends, Appl. Spectosc. 66 (2012) 843–868, https://doi.org/10.1366/12-06681.
[12] M.E. Bosch, A.J.R. Sánchez, F.S. Rojas, C.B. Ojeda, Analytical methodologies for the determination of cisplatin, J. Pharm. Biomed. 47 (2008) 451–459, https://doi.org/10.1016/j.jpba.2008.01.047.
[13] K.H. Laursen, T.H. Hansen, D.P. Persson, J.K. Schjoerring, S. Husted, Multi-elemental fingerprinting of plant tissue by semi-quantitative ICP-MS and chemometrics, J. Anal. At. Spectrom. 24 (2009) 1198–1207, https://doi.org/10.1039/B901960J.
[14] M. Chudzinska, D. Baralkiewicz, Estimation of honey authenticity by multielements characteristics using inductively coupled plasma-mass spectrometry (ICP-MS) combined with chemometrics, Food Chem. 48 (2010) 284–290, https://doi.org/10.1016/j.fct.2009.10.011.
[15] A. Pisani, G. Protano, F. Riccobono, Minor and trace elements in different honey types produced in Siena Country (Italy), Food Chem. 107 (2008) 1553–1560, https://doi.org/10.1016/j.foodchem.2007.09.029.
[16] J.A. Carter, C.S. Long, B.P. Smith, T.L. Smith, G.L. Donati, Combining elemental analysis of toenails and machine learning techniques as a non-invasive diagnostic tool for the robust classification of type-2 diabetes, Expert Syst. Appl. 115 (2019) 245–255, https://doi.org/10.1016/j.eswa.2018.08.002.
[17] Z. Zhou, Y. Chen, M. Ding, P. Wright, Z. Lu, Y. Liu, Analyzing brain networks with PCA and conditional Granger causality, Hum. Brain Mapp. 30 (2009) 2197–2206, https://doi.org/10.1002/hbm.20661.
[18] G. Pasini, Principal component analysis for stock portfolio management, Int. J. Pure Appl. Math. 115 (2017) 153–167, https://doi.org/10.12732/ijpam.v115i1.12.
[19] L. Breiman, Random forests, Mach. Learn. 45 (2001) 5–32, https://doi.org/10.1023/A:1010933404324.
[20] B.A. Goldstein, E.C. Polley, F.B.S. Briggs, Random forests for genetic association studies, Stat. Appl. Genet. Mol. Biol. 10 (2011) 32, https://doi.org/10.2202/1544-6115.1691.
[21] S. Ding, A.J. Pickard, G.L. Kucera, U. Bierbach, Design of enzymatically cleavable prodrugs of a potent platinum-containing anticancer agent, Chem. Eur. J. 20 (2014) 16164–16173, https://doi.org/10.1002/chem.201404675.
[22] A.J. Pickard, F. Liu, T.F. Bartenstein, L.G. Haines, K.E. Levine, G.L. Kucera, U. Bierbach, Redesigning the DNA-targeted chromophore in platinum-acridine anticancer agents: a structure-activity relationship study, Chem. Eur. J. 20 (2014) 16174–16187, https://doi.org/10.1002/chem.201404845.
[23] Y. Akutsu, T. Kono, M. Uesato, I. Hoshino, K. Murakami, T. Fujishiro, S. Imanishi, S. Endo, T. Toyozumi, H. Matsubara, Are additional trace elements necessary in total parental nutrition for patients with esophageal cancer receiving cisplatin-based chemotherapy? Biol. Trace Elem. Res. 150 (2012) 109–115, https://doi.org/10.1007/s12011-012-9513-7.
[24] C.A. Davis, H.S. Nick, A. Agarwal, Manganese superoxide dismutase attenuates cisplatin-induced renal injury: importance of superoxide, J. Am. Soc. Nephrol. 12 (2001) 2683–2690.
[25] I. Sabolic, Common mechanisms in nephropathy induced by toxic metals, Nephron Physiol. 104 (2006) 107–114, https://doi.org/10.1159/000095539.
[26] R.A. van den Berg, H.C.J. Hoefsloot, J.A. Westerhuis, A.K. Smilde, M.J. van der Werf, Centering, scaling, and transformations: improving the biological information content of metabolomics data, BMC Genom. 7 (2006) 142, https://doi.org/10.1186/1471-2164-7-142.
[27] M. Kuhn, K. Johnson, Applied Predictive Modeling, Springer, New York, 2013.
[28] J.A. Gordon, V.G. Gattone II, Mitochondrial alterations in cisplatin-induced acute renal failure, Am. J. Physiol. 250 (1986) F991–F998, https://doi.org/10.1152/ajprenal.1986.250.6.F991.
[29] J.-G. Zhang, W.E. Lindup, Role of calcium in cisplatin-induced cell toxicity in rat renal cortical slices, Toxicol. In Vitro 10 (1996) 205–209, https://doi.org/10.1016/0887-2333(95)00112-3.